DMD Fast Forward. Published on October 2, 2012 as doi:10.1124/dmd.112.047969
This article has not been copyedited and formatted. The final version may differ from this version.

DMD#47969

Title

DNA methylation and histone modification profiles of mouse organic anion transporting polypeptides

Satoki Imai, Ryota Kikuchi, Hiroyuki Kusuhara, and Yuichi Sugiyama

Laboratory of Molecular Pharmacokinetics, Graduate School of Pharmaceutical Sciences, The University of Tokyo (S.I., H.K., R.K.)

Phamacokinetics Research Laboratories, Dainippon Sumitomo Pharma Co., Ltd., 33-94, Enoki-cho, Suita, Osaka, 564-0053, Japan (S.I.)

Sugiyama Laboratory, RIKEN Innovation Center, Research Cluster for Innovation, RIKEN (Y.S.)

Running title: Epigenetic profiles of mouse Oatps

Corresponding Author:

Yuichi Sugiyama, Ph.D.

Address: Sugiyama Laboratory, RIKEN Innovation Center, Research Cluster for Innovation, RIKEN

1-6 Suehiro-cho, Tsurumi-ku, Yokohama City, Kanagawa, 230-0045, Japan

TEL +81-45-506-1814 FAX +81-45-506-1800, Email ychi.sugiyama@riken.jp

The number of text pages: 28

The number of tables: 2,

figures: 4,

references: 29

supplemental tables: 1

The number of words in Abstract: 246,

Introduction: 664

Discussion: 1056

Abbreviations: ChIP, chromatin immunoprecipitation; COBRA, combined bisulfite restriction analysis; HNF, hepatocyte nuclear factor; OAT, organic anion transporter; OATP, organic anion transporting polypeptide; PCR, polymerase chain reaction; RT-PCR, reverse transcription-PCR; SLC, Solute carrier; T-DMR, tissue-dependent differentially methylated region; TSS, transcriptional start site; URAT1, urate transporter 1.

DMD Fast Forward. Published on October 2, 2012 as DOI: 10.1124/dmd.112.047969
This article has not been copyedited and formatted. The final version may differ from this version.

Abstract

Organic anion transporting polypeptides (rodents, Oatps; human, OATPs) are primarily involved in the transmembrane transport of a wide range of endogenous and exogenous compounds. Multiple mouse *Oatp1* isoforms are closely located on chromosome 6 where each isoform shows distinct tissue distribution; Oatp1b2, Oatp1a6 and Oatp1c1 are expressed exclusively in the liver, kidney and cerebrum, respectively; Oatp1a1 in the liver and kidney; and Oatp1a4 in the liver and cerebrum. We have identified tissue-dependent differentially methylated region (T-DMR) around the transcriptional start site (TSS) of *Oatp1b2*, which correlates with its liver-specific expression. Bisulfite sequencing also demonstrated the presence of T-DMRs around the TSS in other *Oatp1* genes, CpG dinucleotides at +149 relative to the TSS for *Oatp1c1*, -48, +101 and +356 for *Oatp1a4*, -572 and -550 for *Oatp1a1*, and -122 and +216 for *Oatp1a6* were differentially methylated among the liver, kidney and cerebrum. These methylation profiles were largely consistent with the tissue distribution of Oatp1 mRNAs. Chromatin immunoprecipitation assay revealed that the mRNA expression of *Oatp1* genes was accompanied by acetylated histone H3. Human *OATP1B1* and *OATP1B3* are located on chromosome 12p12 in the *OATP1* cluster; both show predominant expression in the liver. These genes also contained T-DMRs that were hypomethylated in the liver compared with kidney cortex; -511, -411 and +92 relative to the TSS for *OATP1B1*, and -331, +70 and +73 for *OATP1B3*. These results suggest that the difference in epigenetic profiles comprising DNA methylation and histone acetylation determines the distinct tissue distribution of Oatp/OATP mRNAs.

DMD Fast Forward. Published on October 2, 2012 as DOI: 10.1124/dmd.112.047969
This article has not been copyedited and formatted. The final version may differ from this version.

Introduction

Organic anion transporting polypeptides (rodents, Oatps; human, OATPs) belong to *SLCO* gene superfamily which is comprised of 6 subfamilies. Oatp isoforms classified into the Oatp1 subfamily mediate the sodium-independent transport of various endogenous and exogenous compounds, and they play indispensable roles as xenobiotic detoxification system in the body (Hagenbuch and Gui, 2008). Mouse *Oatp1* genes are located in the chromosome 6 with each isoform exhibiting distinct expression pattern (Fig. 1). Oatp1b2, Oatp1a6, and Oatp1c1 are expressed exclusively in the liver, kidney, and cerebrum, respectively. Oatp1a1 is expressed in the liver and kidney. Oatp1a4 is expressed in the liver and cerebrum (Cheng et al., 2005). *Oatp1a1*, *Oatp1a4*, and *Oatp1a6* show particularly high sequence homology at the amino acid level (> 70%) and also show moderate sequence homology to *Oatp1b2* and *Oatp1c1* (> 40%) (Hagenbuch and Meier, 2003), suggesting that these transporters are products of gene duplication from the same ancestor gene.

The epigenetic systems comprising DNA methylation and histone modification is one of the mechanisms underlying the tissue-specific gene expression (Bird, 2002; Ohgane et al., 2008; Shiota, 2004). Methylation of cytosine residue in the CpG dinucleotide recruits chromatin remodeling factors, such as methyl CpG-binding proteins and histone deacetylases, leading to a transcriptional repression of neighboring genes. Therefore, there is a significant association between the gene expression and DNA methylation/histone acetylation status in the 5′-flanking region. In various types of genes, the widespread existence of tissue-dependent differentially methylated regions (T-DMRs) around their transcription start sites (TSS) has been described, which can potentially explain tissue-specific expression of respective genes (Shiota et al., 2002; Yagi et al., 2008). Recently, we and others have

demonstrated an association of DNA methylation with the tissue-specific expression of human and mouse transporters (Aoki et al., 2008; Imai et al., 2009; Jin et al., 2012; Kikuchi et al., 2007; Kikuchi et al., 2006; Kikuchi et al., 2010). In particular, genome-wide DNA methylation analysis using a methylation-sensitive restriction enzyme HpyCH4IV and mouse promoter tiling array revealed that 53 of 297 *SLC* transporter genes in mouse, including *Oatp1b2/Slco1b2*, were associated with T-DMRtags in the liver (Imai et al., 2009). T-DMRtags in the liver are defined as the HpyCH4IV restriction sites that are hypomethylated in the liver compared with other tissues. Four CpG sites of *Oatp1b2* gene were relatively hypomethylated in the liver compared with kidney and cerebrum, and the difference reached statistical significance at -515 and +115. Based on this finding, we hypothesized that the epigenetic regulations generally govern the distinct tissue distribution of other isoforms in *Oatp1* genes.

Human *OATP1B1* and *OATP1B3*, the counterpart of rodent *Oatp1b2*, reside on chromosome 12p12 in close proximity to other *OATP1* isoforms, *OATP1C1* and *OATP1A2*. OATP1B1 and OATP1B3 are expressed exclusively in the liver. Cumulative clinical evidence shows their importance in the hepatic uptake of a variety of drug such as 3-hydroxy-3-methylglutaryl coenzyme A reductase inhibitors, angiotensin converting enzyme inhibitors, angiotensin receptor II antagonists, and cardiac glycosides, thereby affecting the pharmacological activity and/or adverse event (Giacomini et al., 2010; Hagenbuch and Gui, 2008; Maeda and Sugiyama, 2008). Previously, the promoter regions of *OATP1B1* and *OATP1B3* have been characterized to identify transcription factors responsible for their gene expression (Jung et al., 2001; Ohtsuka et al., 2006). However, the transcription factors, particularly Hepatocyte Nuclear Factor (HNF) 1α, cannot solely account for the liver-specific

expression pattern of these transporters since these transcription factors are also expressed in extrahepatic tissues where their target genes, OATP1B1 and OATP1B3 are not. We hypothesized that epigenetic systems underlie the tissue-specific expression of OATP1B1 and OATP1B3.

The present study was aimed at investigating the involvement of epigenetic systems in the tissue-specific expression of mouse and human *OATP1* genes. We focused on mouse Oatp1 which are expressed in the liver, kidney, and cerebrum (Oatp1a1, Oatp1a4, Oatp1a6, Oatp1b2, and Oatp1c1) and human OATP1B1 and OATP1B3 which are expressed predominantly in the liver. Here we provide clear evidence that the tissue-specific expression of these transporters is associated with epigenetic profiles comprising DNA methylation and histone acetylation around their TSS.

Materials and Methods

Reagents and animals

All reagents were purchased from Wako Pure Chemicals (Osaka, Japan) unless stated otherwise. Male mice of C57BL/6NCrj strain were purchased from Charles River Japan (Kanagawa,. Japan). All mice (11 to 14 weeks) used in this study were maintained under standard conditions and food and water were available ad libitum.

RNA isolation and real-time PCR

Mouse total RNA was isolated from the liver, kidney, and cerebrum using ISOGEN (Nippon Gene, Toyama, Japan) according to the manufacturer's instructions. The RNA was then treated with DNase I to remove the contaminated genomic DNA, followed by reverse transcription (RT) using a random nonamer primer (Takara, Shiga, Japan). The quantitative real-time PCR to detect the partial fragments of Oatp1a1, Oatp1a4, Oatp1a6, Oatp1b2, Oatp1c1, and β-actin cDNA was performed using a LightCycler™ and the appropriate software (version 3; Roche Diagnostics) according to the manufacturer's instructions with the primers shown in Supplemental Table 1. The protocol for PCR was as follows: 95 °C for 30 s; 40 cycles of 95 °C for 5 s, 58 °C for 10 s, and 72 °C for 15 s.

Preparation of brain capillary-enriched fraction

Mouse brain capillary-enriched fraction is prepared as reported previously (Ose et al., 2010). The mouse cerebrum was homogenized using a Polytron homogenizer in 20 volumes (v/w) of ice-cold 0.32 M sucrose (Sigma-Aldrich, St. Louis, MO), and the homogenate was centrifuged at 2,200 g for 10 min. Ten mL of 25% bovine serum albumin was added to the pellet, and the tube was vortexed to suspend the pellet followed by a centrifugation at 2,200 g for 10 min. The pellet was washed by 10 mM Tris-Cl and 0.5 mM

DMD Fast Forward. Published on October 2, 2012 as DOI: 10.1124/dmd.112.047969
This article has not been copyedited and formatted. The final version may differ from this version.

dithiothreitol (pH 7.6) three times and suspended in phosphate buffered saline containing 0.1% protease inhibitor.

Genomic DNA extraction and bisulfite reaction

Human tissue specimens were obtained from non-profit organization Human and Animal Bridging Research Organization (Tokyo, Japan). Human genomic DNA from three individual specimens, and mouse genomic DNA from the liver, kidney, cerebrum, and brain capillary-enriched fraction was extracted using a Get pure DNA Kit (Dojindo Molecular Technologies, Gaithersburg, MD) according to the manufacturer's instructions. One to 10 micrograms of genomic DNA was digested with *Eco*RI (mouse genomic DNA) or *Bam*HI (human genomic DNA) and subjected to the bisulfite reaction as described previously (Kikuchi et al., 2007). The DNA was then precipitated with ethanol, dried, and resuspended in TE buffer (10 mM Tris-HCl, 1 mM EDTA, pH 8.0).

Bisulfite sequencing

The DNA methylation profiles covering the genomic region around the transcriptional start site (TSS) of *Oatp/OATP* transporters were investigated by bisulfite sequencing in mouse liver, kidney, cerebrum, and brain capillary-enriched fraction; and in human liver and kidney cortex. The DNA fragments were amplified by PCR using BIOTAQ^{TM} HS DNA Polymerase (Bioline, London, UK) using the following primers: *Oatp1a1*, –696-F to –305-R and –3-F to +131-R; *Oatp1a4*, –74-F to +261-R and +199-F to +445-R; *Oatp1a6*, –176-F to +363-R; *Oatp1c1*, –275-F to +179-R; *OATP1B1*, –619-F to –263-R and +29-F to +241-R; and *OATP1B3*, –464-F to –303-R and –22-F to +249-R (Supplemental Table 1). The PCR was performed under the following conditions: 94 °C for 10 min; 43 cycles of 94 °C for 30 s, 55 °C (*Oatp1a1*, –3-F/+131-R; *Oatp1a4*, –74-F/+261-R;

Oatp1a4, +199-F/+445-R; *OATP1B1*, –619-F/–263-R; *OATP1B1*, +29-F/+241-R; *OATP1B3*, –464-F/–303-R; and *OATP1B3*, –22-F/+249-R), 57 °C (*Oatp1a6*, –176-F/+363-R; and *Oatp1c1*, –275-F/+179-R), or 60 °C (*Oatp1a1*, –696-F/–305-R) for 30 s, and 72 °C for 1 min; final extension 72 °C for 10 min. The PCR products were cloned into the pGEM-T Easy vector (Promega, Madison, WI), and 10 clones chosen randomly from each sample were sequenced to determine the presence of methylated cytosines. For mouse *Oatps*, differences in the methylation status of each CpG dinucleotide between high- and low-expressing tissues (*i.e.* liver *versus* kidney for *Oatp1a4*, *Oatp1a6* and *Oatp1b2*, liver *versus* cerebrum for *Oatp1a1*, *Oatp1b2* and *Oatp1c1*, and kidney *versus* cerebrum for *Oatp1a1*, *Oatp1a4*, *Oatp1a6*, and *Oatp1c1*) were statistically analyzed using the Quantification tool for Methylation Analysis (QUMA; http://quma.cdb.riken.jp/) (Kumaki et al., 2008) with Fisher's exact test followed by Bonferroni adjustment to correct for multiple testing. Significant differences ($P < 0.05$) between the two tissues were denoted by * (liver *versus* kidney), † (liver *versus* cerebrum), and ‡ (kidney *versus* cerebrum). For human *OATP1B1* and *OATP1B3*, the degree of methylation was calculated at each CpG dinucleotide in individual specimens, and these values were statistically compared between the two tissues using Student's t-test. Significant differences ($P < 0.05$) between the liver and kidney cortex were denoted by asterisks. The degree of DNA methylation in the entire region was determined by dividing the total number of methylated CpGs by that of all CpGs analyzed in bisulfite sequencing. Differences in the methylation status of entire region between high- and low-expressing tissues were statistically analyzed using Fisher's exact test followed by Bonferroni adjustment.

DMD Fast Forward. Published on October 2, 2012 as DOI: 10.1124/dmd.112.047969
This article has not been copyedited and formatted. The final version may differ from this version.

Combined bisulfite restriction analysis

The DNA methylation profiles of the CpG dinucleotides at –572 bp, +101 bp, +216 bp, –175 bp, –411 bp, and +73 bp relative to the TSS of *Oatp1a1*, *Oatp1a4*, *Oatp1a6*, *Oatp1c1*, *OATP1B1*, and *OATP1B3*, respectively, were investigated by combined bisulfite restriction analysis (COBRA) (Xiong and Laird, 1997). The DNA fragments were amplified by PCR as described above using the following primers: *Oatp1a1*, –696-F to –305-R; *Oatp1a4*, –74-F to +261-R; *Oatp1a6*, –176-F to +363-R; *Oatp1c1*, –275-F to +179-R; *OATP1B1*, –619-F to –263-R; and *OATP1B3*, –22-F to +249-R (Supplemental Table 1). The PCR fragments were digested with HpyCH4IV (New England Biolabs, Beverly, MA) for *Oatp1a1*, *Oatp1a4*, *Oatp1a6*, *Oatp1c1*, and *OATP1B1*, or TaqI (Takara, Shiga, Japan) for *OATP1B3*. Because only unmethylated cytosine residues are converted to thymines by the bisulfite reaction, PCR fragments from unmethylated genomic DNA are resistant to restriction enzyme digestion, whereas those from methylated DNA are digested.

Chromatin immunoprecipitation assay

The chromatin immunoprecipitation (ChIP) assay was performed using anti-acetylated histone H3 antibody (Upstate Biotechnology, Lake Placid, NY) according to a procedure described previously (Imai et al., 2009). Normal rabbit IgG was used as a negative control to verify the immunoprecipitation specificity. Briefly, ca. 250 mg of liver, kidney, and cerebrum from 11-week-old male C57BL/6NCrj mice was chopped into small pieces and treated with 1% formaldehyde to form DNA–protein cross-links. The samples were homogenized, treated with cell lysis buffer, and centrifuged to precipitate the nuclei. The nuclei were then lysed with nuclei lysis buffer and sonicated on ice. The samples were preincubated with salmon sperm DNA/Protein A-agarose suspension to reduce the

nonspecific background, and the samples were incubated with an antibody against acetylated histone H3, normal rabbit IgG, or an equivalent amount of PBS as the 'no antibody' sample at 4 ℃ overnight. The samples were then mixed with salmon sperm DNA/Protein A-agarose suspension, rotated for 60 min at 4 ºC, and centrifuged at 20,000 g for 1 min at 4 ºC. DNA was purified from the precipitated immune complex after extensive washing and reversing of the DNA–protein cross-links. The supernatant from the 'no antibody' sample was collected as the 'total input'. The quantitative real-time PCR was performed using a LightCycler™ and the appropriate software (version 3; Roche Diagnostics) according to the manufacturer's instructions with the primers shown in Supplemental Table 1. The protocol for PCR was as follows: 95 °C for 30 s; 40 cycles of 95 °C for 5 s, 58 °C for 10 s, and 72 °C for 15 s. The enrichment of DNA in the immunoprecipitates was calculated relative to the 1:100 diluted 'total input' samples. Statistical significance was assessed between tissues using one-way analysis of variance followed by Tukey's multiple comparison post hoc test. Significant differences ($P < 0.05$) between the tissues were denoted by asterisks.

Results

mRNA expression profiles of the mouse Oatps

The mRNA expression of Oatp1c1, Oatp1b2, Oatp1a4, Oatp1a1, and Oatp1a6 in the mouse liver, kidney, and cerebrum was quantified by real-time PCR (Fig. 1B). The results confirmed that Oatp1b2, Oatp1a6 and Oatp1c1 are expressed predominantly in the liver, kidney and cerebrum, respectively. Oatp1a1 was expressed in the liver and kidney while the expression in the cerebrum was negligible, and Oatp1a4 was expressed in the liver and cerebrum and minimal expression was observed in the kidney. These distinct tissue distribution patterns of mouse Oatp1 mRNA are consistent with those reported previously (Cheng et al., 2005).

DNA methylation profiles around the transcriptional start site of mouse *Oatp1* genes

The DNA methylation profiles of the CpG dinucleotides from -600 to +400 relative to the TSS of mouse *Oatp1* genes were determined in the liver, kidney and cerebrum (Fig. 2). The degree of DNA methylation in these regions was calculated and compared among the tissues (Table 1). The corresponding data for *Oatp1b2* were cited from our previous study (Imai et al., 2009) for comparison. In *Oatp1c1*, one CpG site located at +149 relative to the TSS was regarded as T-DMR while the other two sites upstream of the TSS were similarly methylated among tissues (Fig. 2B). In *Oatp1a4*, two out of six CpG sites downstream the TSS (+101 and +356) and one site upstream the TSS (-48) constitute the T-DMRs. *Oatp1a4* was largely and moderately methylated in the kidney and cerebrum, respectively, while only slightly methylated in the liver. In *Oatp1a1*, two CpG sites in the upstream of the TSS (-572 and -550) were identified as T-DMRs while the degree of methylation at +59 CpG site was not statistically different between the tissues. *Oatp1a1* was moderately to largely

DMD Fast Forward. Published on October 2, 2012 as DOI: 10.1124/dmd.112.047969
This article has not been copyedited and formatted. The final version may differ from this version.

methylated in the kidney and cerebrum while significantly hypomethylated in the liver. In *Oatp1a6,* both the upstream and downstream CpG sites around the TSS (-122 and +216) were differentially methylated among tissues. *Oatp1a6* was moderately to largely hypermethylated in the liver and cerebrum, while significantly hypomethylated in the kidney. The DNA methylation in the brain capillary-enriched fraction was also investigated for *Oatp1c1* and *Oatp1a4* which are known to be localized in the mouse brain capillaries (Ose et al., 2010; Tohyama et al., 2004). Most of the CpG dinucleotides are relatively hypomethylated in the brain capillaries, being consistent with the mRNA expression of these transporters. The combined bisulfite restriction analysis corroborated the results of bisulfite sequencing for the DNA methylation status of CpG dinucleotides located at –572 bp, +101 bp and –175 bp relative to the TSS of *Oatp1a1*, *Oatp1a4* and *Oatp1c1*, respectively (Fig. 2C). Although the difference in DNA methylation was less apparent in COBRA than bisulfite sequencing at +216 CpG dinucleotide in *Oatp1a6*, it was qualitatively similar to each other where the site is relatively hypomethylated in the kidney compared with the other two tissues.

Histone acetylation profiles in the promoter region of mouse *Oatp* transporters

ChIP assays were performed to examine the histone H3 acetylation profiles of mouse Oatp transporters (Fig. 3). The corresponding data for *Oatp1b2* were cited from our previous study (Imai et al., 2009) for comparison. The histone H3 around the TSS of *Oatp1c1* was hyperacetylated in the cerebrum, while the acetylation in the liver and kidney was minimal. Similarly, *Oatp1b2* and *Oatp1a1* were hyperacetylated only in the liver. *Oatp1a4* was hyperacetylated in the liver and cerebrum but not in the kidney. Acetylation of histone H3 was not observed for *Oatp1a6* in these tissues.

DNA methylation profiles around the transcriptional start site of human *OATP1B1* and

DMD Fast Forward. Published on October 2, 2012 as DOI: 10.1124/dmd.112.047969
This article has not been copyedited and formatted. The final version may differ from this version.

OATP1B3

The DNA methylation profiles of CpG dinucleotides around the TSS of *OATP1B1* and *OATP1B3* were determined in three individual specimens of human liver and kidney cortex (Fig. 4). The CpG sites at -511, -411, and +92 relative to the TSS for *OATP1B1*, and those at -331, +70 and +73 for *OATP1B3* were significantly hypomethylated in the liver compared with the kidney cortex and regarded as T-DMRs. The degree of DNA methylation in these regions was calculated and compared among the tissues (Table 2). The CpG dinucleotides around the TSS of *OATP1B1* and *OATP1B3* were overall significantly hypomethylated in the liver compared with the kidney cortex. The DNA methylation status examined by COBRA for the CpG dinucleotides at –411 bp and +73 bp relative to the TSS of *OATP1B1* and *OATP1B3*, respectively, corroborated the results of bisulfite sequencing (Fig. 4C).

DMD Fast Forward. Published on October 2, 2012 as DOI: 10.1124/dmd.112.047969
This article has not been copyedited and formatted. The final version may differ from this version.

Discussion

In the present study, we investigated the DNA methylation and histone acetylation profiles of mouse and human *Oatp1/OATP1* genes, which are localized on the same chromosome within close proximity, as a mechanism underlying their tissue specific expression.

Consistent with previous report (Cheng et al., 2005), the Oatp1 isoforms showed distinct tissue distribution (Fig. 1). Bisulfite genomic sequencing located a number of CpG dinucleotides differentially methylated between tissues around the TSS of mouse *Oatp1* genes (Fig. 2), where the difference in the DNA methylation status is in good agreement with the mRNA expression profiles of respective transporters. DNA methylation status of the entire region around the TSS was largely consistent with the mRNA expression of respective genes (Table 1). The CpG dinucleotides were hypomethylated (<30% of methylation) in most of the transporter-expressing tissues, *i.e. Oatp1b2*, *Oatp1a4*, and *Oatp1a1* in the liver, *Oatp1a6* in the kidney, and *Oatp1c1* and *Oatp1a4* in the brain capillary-enriched fraction, whereas those were moderately (30-70%) to largely (>70%) methylated in non-expressing tissues, *i.e. Oatp1c1* and *Oatp1a6* in the liver, *Oatp1c1*, *Oatp1b2* and *Oatp1a4* in the kidney, and *Oatp1b2*, *Oatp1a1* and *Oatp1a6* in the cerebrum. There were some discrepancies between the mRNA expression and DNA methylation status, i.e. *Oatp1a1* was moderately methylated (60%) in the kidney, and *Oatp1c1* and *Oatp1a4* were moderately methylated (37% and 51%, respectively) in the cerebrum. This could be ascribed to the regional expression of Oatp1a1 in the kidney, and Oatp1c1 and Oatp1a4 in the cerebrum, where the expression is restricted to the proximal tubules (Oatp1a1) (Bergwerk et al., 1996) and brain capillaries (Oatp1c1 and Oatp1a4) (Ose et al., 2010; Tohyama et al., 2004). Indeed, the

DMD Fast Forward. Published on October 2, 2012 as DOI: 10.1124/dmd.112.047969
This article has not been copyedited and formatted. The final version may differ from this version.

CpG dinucleotides around the TSS of *Oatp1c1* and *Oatp1a4* tend to be methylated to the lesser extent in the brain capillary-enriched fraction compared with the cerebrum. These results suggest that the tissue-specific expression of these transporters is regulated through DNA methylation-dependent gene silencing together with transcription factors. Generally, DNA methylation status is linked tightly with the histone acetylation status and activated genes are associated with acetylated histone H3. Subsequent ChIP assays revealed that histone acetylation was associated with the expression of mouse *Oatp1* genes except for *Oatp1a1* and *Oatp1a6*, of which histone H3 around the TSS was not acetylated in the kidney regardless of their expression (Fig. 3). In the kidney, Oatp1a1 is exclusively expressed in proximal tubules (Bergwerk et al., 1996). It is possible that histone H3 around the TSS of *Oatp1a1* is acetylated only in the proximal tubules, which could be masked when ChIP was performed using whole kidney. Indeed, Oatp1a1 expression was associated with acetylated histone H3 in the liver which mainly consists of a single type of cells, hepatocyte. Regional expression of Oatp1a6 in the kidney has not been investigated. Nevertheless, the mRNA expression of mouse *Oatp1* genes is associated with either DNA methylation or histone acetylation or both in most cases, indicating the role of epigenetic regulation in the distinct expression pattern of these genes.

The high sequence identity of mouse *Oatp1* genes suggests that they are the products of genetic duplication from the same ancestor gene. Gene duplication is regarded as a key mechanism for the evolution of new genes (Ohno, 1970). The connection between gene duplication and epigenetic modifications has not been well established (Zheng, 2008), and to our knowledge, there are few systematic studies investigating the epigenetic regulation of duplicated genes. Rodin and Riggs proposed an epigenetic complementation model where

duplicated genes are epigenetically silenced in a tissue-complementary manner, exposing each of the duplicates to negative selection, thus protecting from pseudogenization (Rodin and Riggs, 2003). Recently, DNA methylation status of the mouse prolactin superfamily was analyzed and it was suggested that the methylation is involved in the tissue-specific expression and sequence diversity during evolution (Hayakawa et al., 2012), which is similar to our present findings. Taken together, it is plausible that the epigenetic profiles differentiate the mouse *Oatp1* genes in terms of their tissue distributions during the gene duplication events.

We and others have revealed the involvement of DNA methylation-dependent gene silencing in the tissue-specific expression of transporters in humans and mice (Douet et al., 2007; Imai et al., 2009; Jin et al., 2012; Kikuchi et al., 2007; Kikuchi et al., 2010). Both human and mouse *OAT1*/*Oat1* is hypomethylated in the kidney while hypermethylated in the liver around the TSS (Jin et al., 2012). On the other hand, most of the CpGs in the 5'-flanking region of human *OAT3* is hypermethylated in the liver and hypomethylated in the kidney while T-DMR is not prevalent in mouse *Oat3*, and vice versa for human and mouse *URAT1* genes; mouse but not human *Urat1* genes contained a T-DMR associated with the tissue-specific mRNA expression. This motivated us to investigate the DNA methylation profile in human counterparts of mouse *Oatp1* genes. Consistent with *Oatp1b2* in mouse, both human *OATP1B1* and *OATP1B3* genes contained T-DMRs which were hypomethylated in the liver, but hypermethylated in the kidney (Fig. 4 and Table 2). Since the promoters of human *OATP1B1*, *OATP1B3* and mouse *Oatp1b2* are activated by the same transcription factor, HNF1α (Jung et al., 2001; Maher et al., 2006), it is most likely that DNA demethylation of these genes in the liver evokes the acetylation of histone H3, which allows

HNF1α to bind to its recognition sites and activate the promoters. The same regulatory cascade has been proposed for the kidney-specific expression of organic anion transporters and amino acid transporters (Jin et al., 2012; Kikuchi et al., 2010). As reported previously for *OAT4* and *URAT1* promoters (Jin et al., 2012), the methylation profiles of *OATP1B1* and *OATP1B3* in the liver had a moderate batch difference; hypomethylated in Liver-1, whereas moderately methylated in Liver-2 and -3 (Fig. 4B). It is possible that this leads to the interindividual differences in the mRNA expression, and consequently to the in vivo transport activities. Further studies are necessary to elucidate the association, and its impact on the pharmacokinetics of drugs.

In conclusion, we have demonstrated a clear association between the tissue-specific expression and epigenetic profiles comprising DNA methylation and histone acetylation for *Oatp1a1*, *Oatp1a4*, *Oatp1a6*, *Oatp1b2*, and *Oatp1c1* in mice, and *OATP1B1* and *OATP1B3* in human. It is likely that the difference in the epigenetic profiles underlies the distinct tissue distribution of each of the Oatp/OATP family transporters which seem to be evolved from the same ancestor genes.

Authorship Contributions

Participated in research design: Imai, Kikuchi, Kusuhara, and Sugiyama.

Conducted experiments: Imai.

Performed data analysis: Imai, Kikuchi, and Kusuhara.

Wrote or contributed to the writing of the manuscript: Imai, Kikuchi, Kusuhara, and Sugiyama.

References

Aoki M, Terada T, Kajiwara M, Ogasawara K, Ikai I, Ogawa O, Katsura T, and Inui K (2008) Kidney-specific expression of human organic cation transporter 2 (OCT2/SLC22A2) is regulated by DNA methylation. *Am J Physiol Renal Physiol* **295**: F165-170.

Bergwerk AJ, Shi X, Ford AC, Kanai N, Jacquemin E, Burk RD, Bai S, Novikoff PM, Stieger B, Meier PJ, Schuster VL, and Wolkoff AW (1996) Immunologic distribution of an organic anion transport protein in rat liver and kidney. *Am J Physiol* **271**: G231-238.

Bird A (2002) DNA methylation patterns and epigenetic memory. *Genes Dev* **16**: 6-21.

Cheng X, Maher J, Chen C, and Klaassen CD (2005) Tissue distribution and ontogeny of mouse organic anion transporting polypeptides (Oatps). *Drug Metab Dispos* **33**: 1062-1073.

Douet V, Heller MB, and Le Saux O (2007) DNA methylation and Sp1 binding determine the tissue-specific transcriptional activity of the mouse Abcc6 promoter. *Biochem Biophys Res Commun* **354**: 66-71.

Giacomini KM, Huang SM, Tweedie DJ, Benet LZ, Brouwer KL, Chu X, Dahlin A, Evers R, Fischer V, Hillgren KM, Hoffmaster KA, Ishikawa T, Keppler D, Kim RB, Lee CA, Niemi M, Polli JW, Sugiyama Y, Swaan PW, Ware JA, Wright SH, Yee SW, Zamek-Gliszczynski MJ, and Zhang L (2010) Membrane transporters in drug development. *Nat Rev Drug Discov* **9**: 215-236.

Hagenbuch B, and Gui C (2008) Xenobiotic transporters of the human organic anion transporting polypeptides (OATP) family. *Xenobiotica* **38**: 778-801.

Hagenbuch B, and Meier PJ (2003) The superfamily of organic anion transporting polypeptides. *Biochim Biophys Acta* **1609**: 1-18.

Hayakawa K, Nakanishi MO, Ohgane J, Tanaka S, Hirosawa M, Soares MJ, Yagi S, and Shiota K (2012) Bridging sequence diversity and tissue-specific expression by DNA methylation in genes of the mouse prolactin superfamily. *Mamm Genome* 23:336-45.

Imai S, Kikuchi R, Kusuhara H, Yagi S, Shiota K, and Sugiyama Y (2009) Analysis of DNA methylation and histone modification profiles of liver-specific transporters. *Mol Pharmacol* **75**: 568-576.

Jin L, Kikuchi R, Saji T, Kusuhara H, and Sugiyama Y (2012) Regulation of tissue-specific expression of renal organic anion transporters by hepatocyte nuclear factor 1 alpha/beta and DNA methylation. *J Pharmacol Exp Ther* **340**: 648-655.

Jung D, Hagenbuch B, Gresh L, Pontoglio M, Meier PJ, and Kullak-Ublick GA (2001) Characterization of the human OATP-C (SLC21A6) gene promoter and regulation of

liver-specific OATP genes by hepatocyte nuclear factor 1 alpha. *J Biol Chem* **276**: 37206-37214.

Kikuchi R, Kusuhara H, Hattori N, Kim I, Shiota K, Gonzalez FJ, and Sugiyama Y (2007) Regulation of tissue-specific expression of the human and mouse urate transporter 1 gene by hepatocyte nuclear factor 1 alpha/beta and DNA methylation. *Mol Pharmacol* **72**: 1619-1625.

Kikuchi R, Kusuhara H, Hattori N, Shiota K, Kim I, Gonzalez FJ, and Sugiyama Y (2006) Regulation of the expression of human organic anion transporter 3 by hepatocyte nuclear factor 1alpha/beta and DNA methylation. *Mol Pharmacol* **70**: 887-896.

Kikuchi R, Yagi S, Kusuhara H, Imai S, Sugiyama Y, and Shiota K (2010) Genome-wide analysis of epigenetic signatures for kidney-specific transporters. *Kidney Int* **78**: 569-577.

Kumaki Y, Oda M, and Okano M (2008) QUMA: quantification tool for methylation analysis. *Nucleic Acids Res* **36**: W170-175.

Maeda K, and Sugiyama Y (2008) Impact of genetic polymorphisms of transporters on the pharmacokinetic, pharmacodynamic and toxicological properties of anionic drugs. *Drug Metab Pharmacokinet* **23**: 223-235.

Maher JM, Slitt AL, Callaghan TN, Cheng X, Cheung C, Gonzalez FJ, and Klaassen CD (2006) Alterations in transporter expression in liver, kidney, and duodenum after targeted disruption of the transcription factor HNF1alpha. *Biochem Pharmacol* **72**: 512-522.

Ohgane J, Yagi S, and Shiota K (2008) Epigenetics: the DNA methylation profile of tissue-dependent and differentially methylated regions in cells. *Placenta* **29 Suppl A**: S29-35.

Ohno S (1970) Evolution by gene duplication., Springer, Berlin.

Ohtsuka H, Abe T, Onogawa T, Kondo N, Sato T, Oshio H, Mizutamari H, Mikkaichi T, Oikawa M, Rikiyama T, Katayose Y, and Unno M (2006) Farnesoid X receptor, hepatocyte nuclear factors 1alpha and 3beta are essential for transcriptional activation of the liver-specific organic anion transporter-2 gene. *J Gastroenterol* **41**: 369-377.

Ose A, Kusuhara H, Endo C, Tohyama K, Miyajima M, Kitamura S, and Sugiyama Y (2010) Functional characterization of mouse organic anion transporting peptide 1a4 in the uptake and efflux of drugs across the blood-brain barrier. *Drug Metab Dispos* **38**: 168-176.

Rodin SN, and Riggs AD (2003) Epigenetic silencing may aid evolution by gene duplication. *J Mol Evol* **56**: 718-729.

Shiota K (2004) DNA methylation profiles of CpG islands for cellular differentiation and development in mammals. *Cytogenet Genome Res* **105**: 325-334.

Shiota K, Kogo Y, Ohgane J, Imamura T, Urano A, Nishino K, Tanaka S, and Hattori N (2002) Epigenetic marks by DNA methylation specific to stem, germ and somatic cells in mice. *Genes Cells* **7**: 961-969.

Tohyama K, Kusuhara H, and Sugiyama Y (2004) Involvement of multispecific organic anion transporter, Oatp14 (Slc21a14), in the transport of thyroxine across the blood-brain barrier. *Endocrinology* **145**: 4384-4391.

Xiong Z, and Laird PW (1997) COBRA: a sensitive and quantitative DNA methylation assay. *Nucleic Acids Res* **25**: 2532-2534.

Yagi S, Hirabayashi K, Sato S, Li W, Takahashi Y, Hirakawa T, Wu G, Hattori N, Ohgane J, Tanaka S, Liu XS, and Shiota K (2008) DNA methylation profile of tissue-dependent and differentially methylated regions (T-DMRs) in mouse promoter regions demonstrating tissue-specific gene expression. *Genome Res* **18**: 1969-1978.

Zheng D (2008) Gene duplication in the epigenomic era. *Epigenetics* **3**: 250-253.

Footnote

This study was supported by the Japan Society for the Promotion of Science [Grant-in-Aid for Scientific Research (S) 24229002, Scientific Research (B) 23390034, and Grant-in-Aid for Challenging Exploratory Research 21659037].

[1]Current Affiliation:

Ryota Kikuchi, Drug Metabolism, Developmental Sciences, Global Pharmaceutical Research and Development, Abbott Laboratories, Abbott Park, IL 60064, USA

Legends for Figures

Fig. 1. mRNA expression profiles of the mouse *Oatp* transporter genes.

(A) Gene loci of mouse *Oatp1* transporters on chromosome 6. (B) mRNA expression profiles of the mouse *Oatp1* genes. mRNA of Oatp1a1, Oatp1a4, Oatp1a6, Oatp1b2, and Oatp1c1 in mouse liver, kidney, and cerebrum was quantified by real-time PCR using specific primers (Supplemental Table 1) as described in Materials and Methods. The mRNA expression levels are represented as a ratio to that of β-actin in each tissue. The results are presented as the mean value of two independent measurements for cDNAs derived from a single animal.

Fig. 2. DNA methylation profiles around the transcriptional start site of the mouse *Oatp1* genes.

Bisulfite genomic sequencing analysis and COBRA were performed for *Oatp1c1*, *Oatp1a4*, *Oatp1a1*, and *Oatp1a6* with genomic DNA extracted from mouse liver, kidney, cerebrum, and brain capillary-enriched fraction as described in Materials and Methods. The data for *Oatp1b2* obtained previously (Imai et al., 2009) was also presented for comparison. (A) Schematic diagrams of the genomic region around the transcriptional start site (TSS). The vertical lines and numbers indicate the positions of the cytosine residues of the CpG dinucleotides relative to the TSS (+1). (B) DNA methylation status of individual CpG dinucleotides. The open and closed circles represent unmethylated and methylated cytosines, respectively. Significant differences ($P < 0.05$) between the two samples were denoted by * (liver *versus* kidney), † (liver *versus* cerebrum), and ‡ (kidney *versus* cerebrum). (C) Combined bisulfite restriction analysis. The bisulfite PCR products were digested with

HpyCH4IV and electrophoresed on a 2.0% agarose gel to evaluate the methylation status of the CpG dinucleotides. The conditions of undigested (–) and digested (+) are indicated on the top of the gel.

Fig. 3. Histone acetylation profiles around the transcriptional start site of the mouse *Oatp1* genes.

The histone H3 acetylation status of *Oatp1c1*, *Oatp1a4*, *Oatp1a1*, and *Oatp1a6* around the transcriptional start site was determined by ChIP assay in mouse liver, kidney, and cerebrum as described in Materials and Methods. The data for *Oatp1b2* and *β-actin* obtained in our previous study (Imai et al., 2009) was also presented for comparison. The closed columns represent the histone acetylation of each sample relative to its respective total input. Normal rabbit IgG was included as a negative control to verify the immunoprecipitation specificity (open columns). The results are presented as the mean ± SD of triplicate experiments. Significant differences ($P < 0.05$) between the tissues were denoted by asterisks.

Fig. 4. DNA methylation profiles around the transcriptional start site of *OATP1B1* and *OATP1B3*.

Bisulfite genomic sequencing analysis and COBRA were performed for *OATP1B1* and *OATP1B3* with genomic DNA extracted from human liver and kidney cortex as described in Materials and Methods. (A) Schematic diagrams of the genomic region around the transcriptional start site (TSS). The vertical lines and numbers indicate the positions of the cytosine residues of the CpG dinucleotides relative to the TSS (+1). (B) DNA methylation status of individual CpG dinucleotides. The open and closed circles represent unmethylated

and methylated cytosines, respectively. Significant differences ($P < 0.05$) between the liver and kidney cortex were denoted by asterisks. (C) Combined bisulfite restriction analysis. The bisulfite PCR products were digested with HpyCH4IV (*OATP1B1*) or TaqI (*OATP1B3*) and electrophoresed on a 2.0% agarose gel to evaluate the methylation status of the CpG dinucleotides. The conditions of undigested (–) and digested (+) are indicated on the top of the gel.

DMD Fast Forward. Published on October 2, 2012 as DOI: 10.1124/dmd.112.047969
This article has not been copyedited and formatted. The final version may differ from this version.

Tables

Table 1: The degree of DNA methylation around the TSS of mouse *Oatps*

The percentage was calculated by dividing the total number of methylated CpGs by that of all CpGs analyzed in bisulfite sequencing. Differences in the methylation status of entire region between the tissues were statistically analyzed using Fisher's exact test followed by Bonferroni adjustment to correct for multiple testing. Significant differences ($P < 0.05$) between the two tissues were denoted by * (liver *versus* kidney), † (liver *versus* cerebrum), and ‡ (kidney *versus* cerebrum).

The degree of DNA methylation (%)					
	Oatp1c1	*Oatp1b2*	*Oatp1a4*	*Oatp1a1*	*Oatp1a6*
Liver	60	20	26	27	85
Kidney	50	73	73	60	20
Cerebrum	37	88	51	80	65
Brain capillary-enriched fraction	20	-	26	-	-
Statistical analysis		* †	* ‡	†	* ‡

DMD Fast Forward. Published on October 2, 2012 as DOI: 10.1124/dmd.112.047969
This article has not been copyedited and formatted. The final version may differ from this version.

Table 2: The degree of DNA methylation around the TSS of human *OATP1B1* and *OATP1B3*

The percentage was calculated by dividing the total number of methylated CpGs by that of all CpGs analyzed in bisulfite sequencing. Differences in the methylation status of entire region between the tissues were statistically analyzed using Fisher's exact test. Significant differences ($P < 0.05$) between the liver and kidney cortex were denoted by asterisks.

The degree of DNA methylation (%)		
	OATP1B1	*OATP1B3*
Liver	41	37
Kidney cortex	89	88
Statistical analysis	*	*

Fig. 1

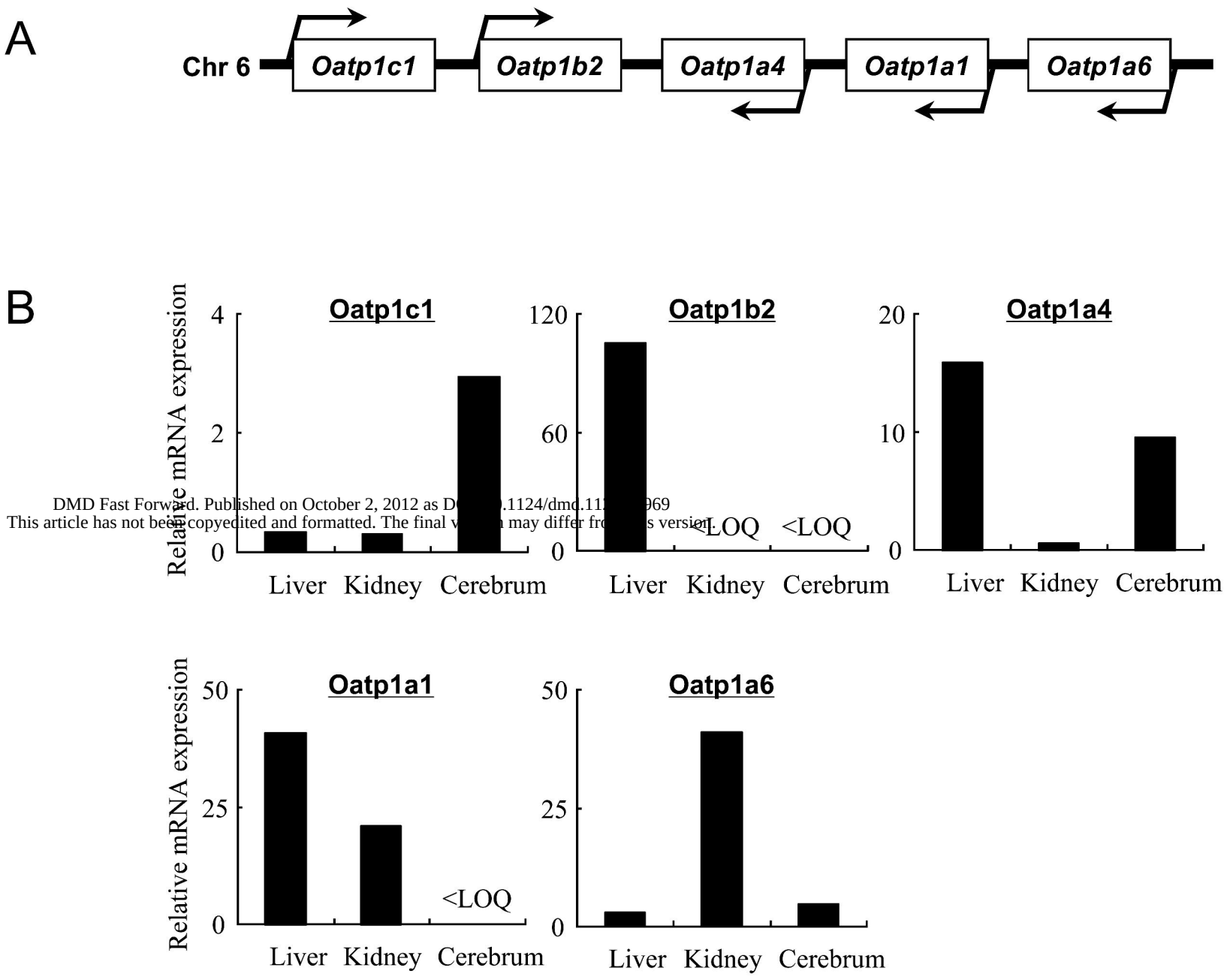

Fig. 2 A

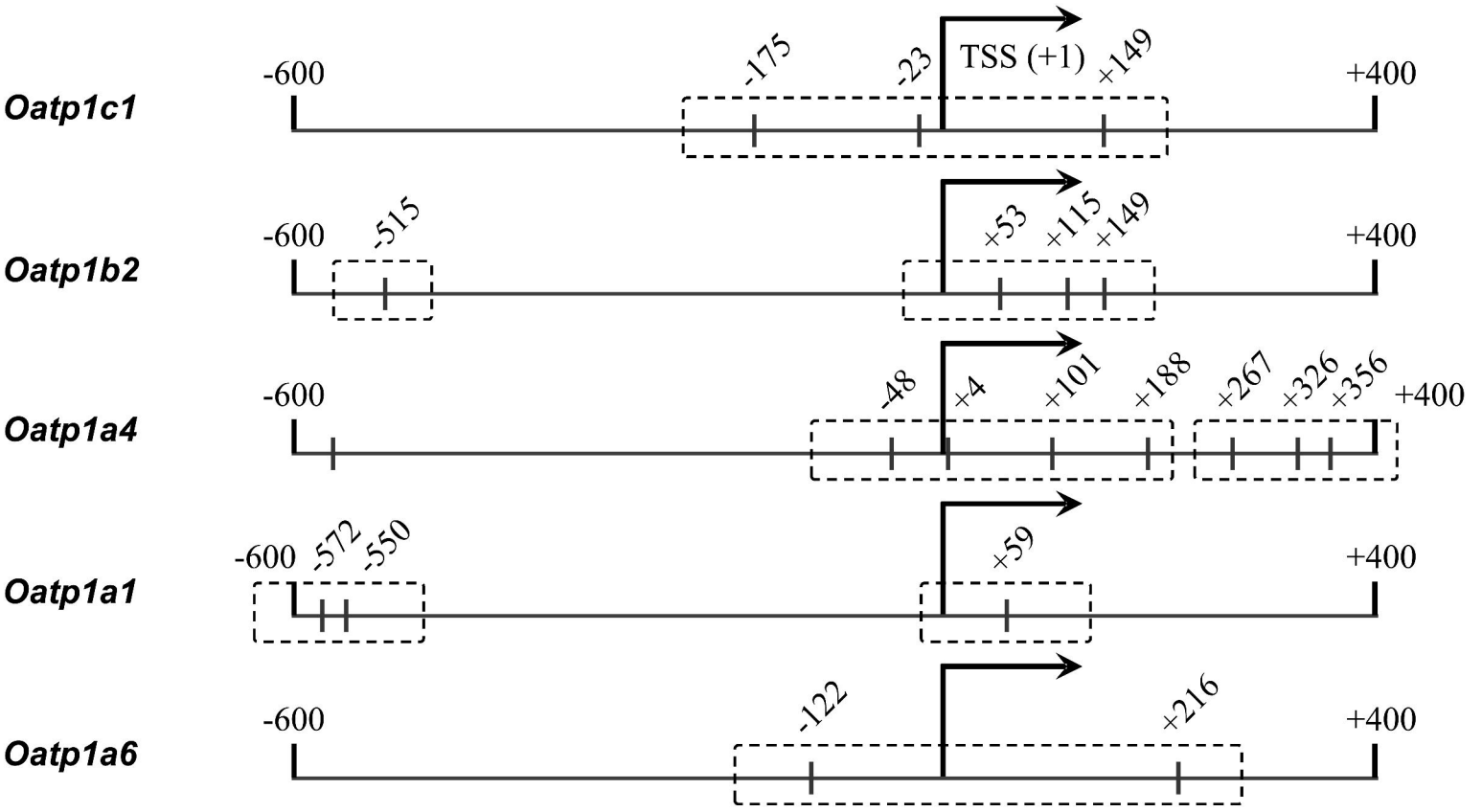

B

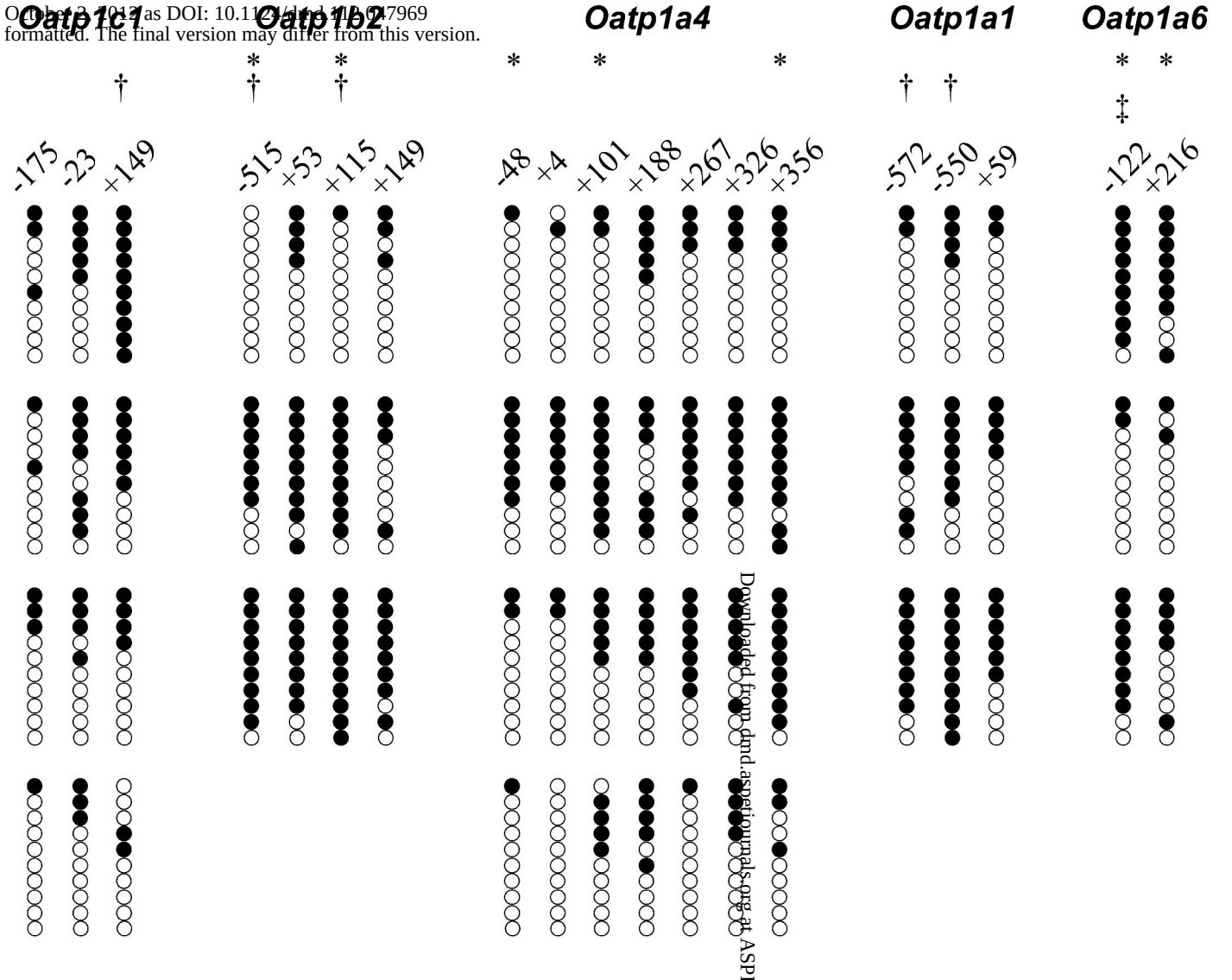

C

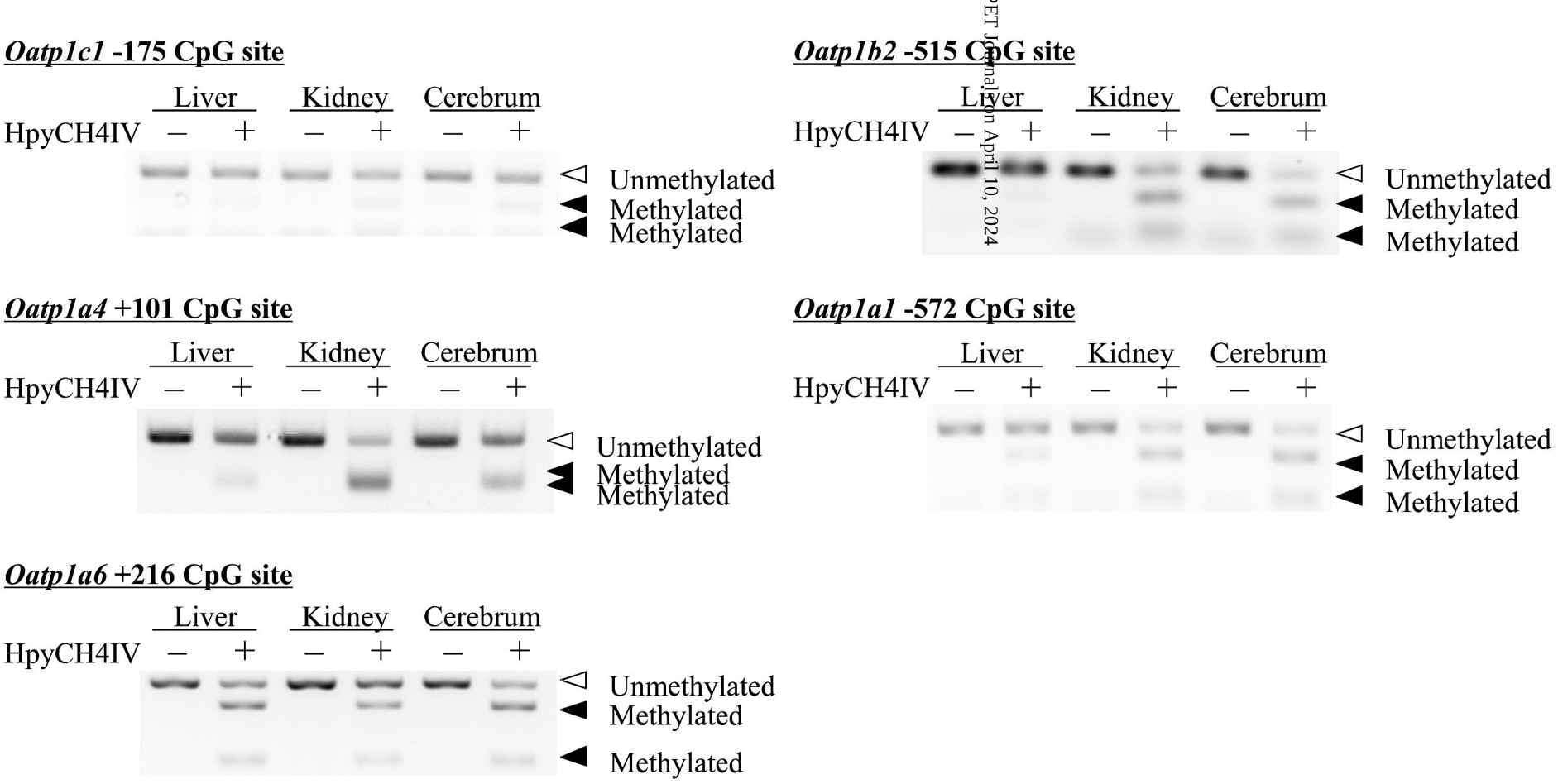

Fig. 3

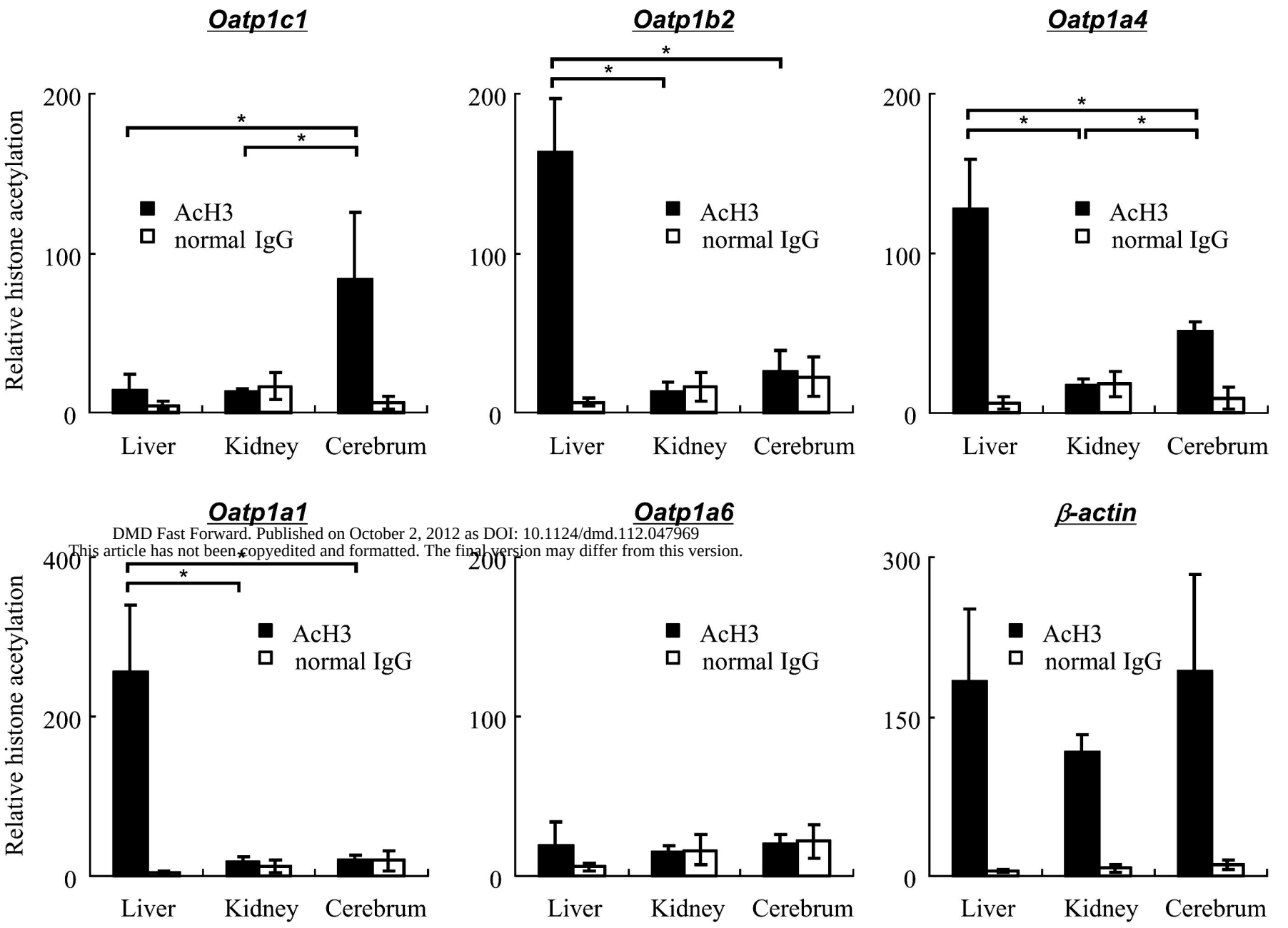

DMD Fast Forward. Published on October 2, 2012 as DOI: 10.1124/dmd.112.047969

Fig. 4 A

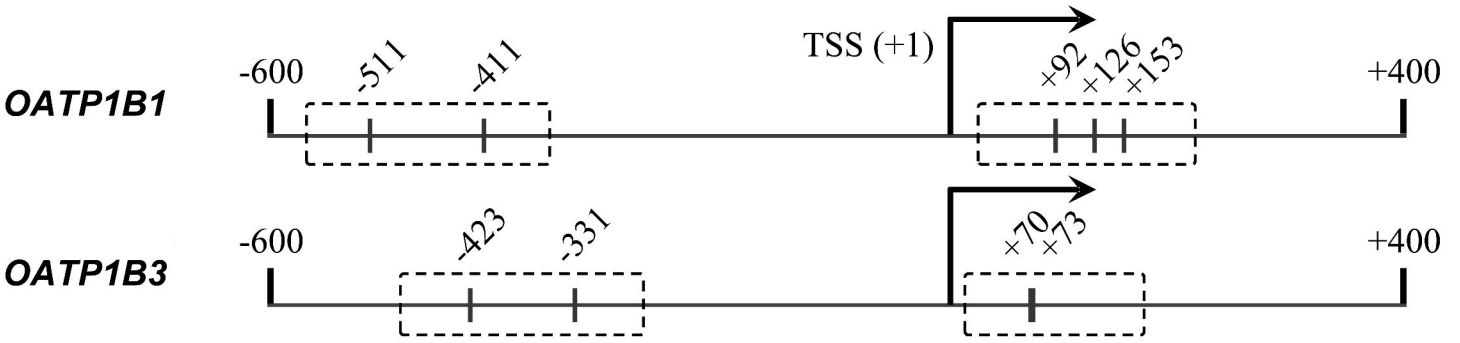

B

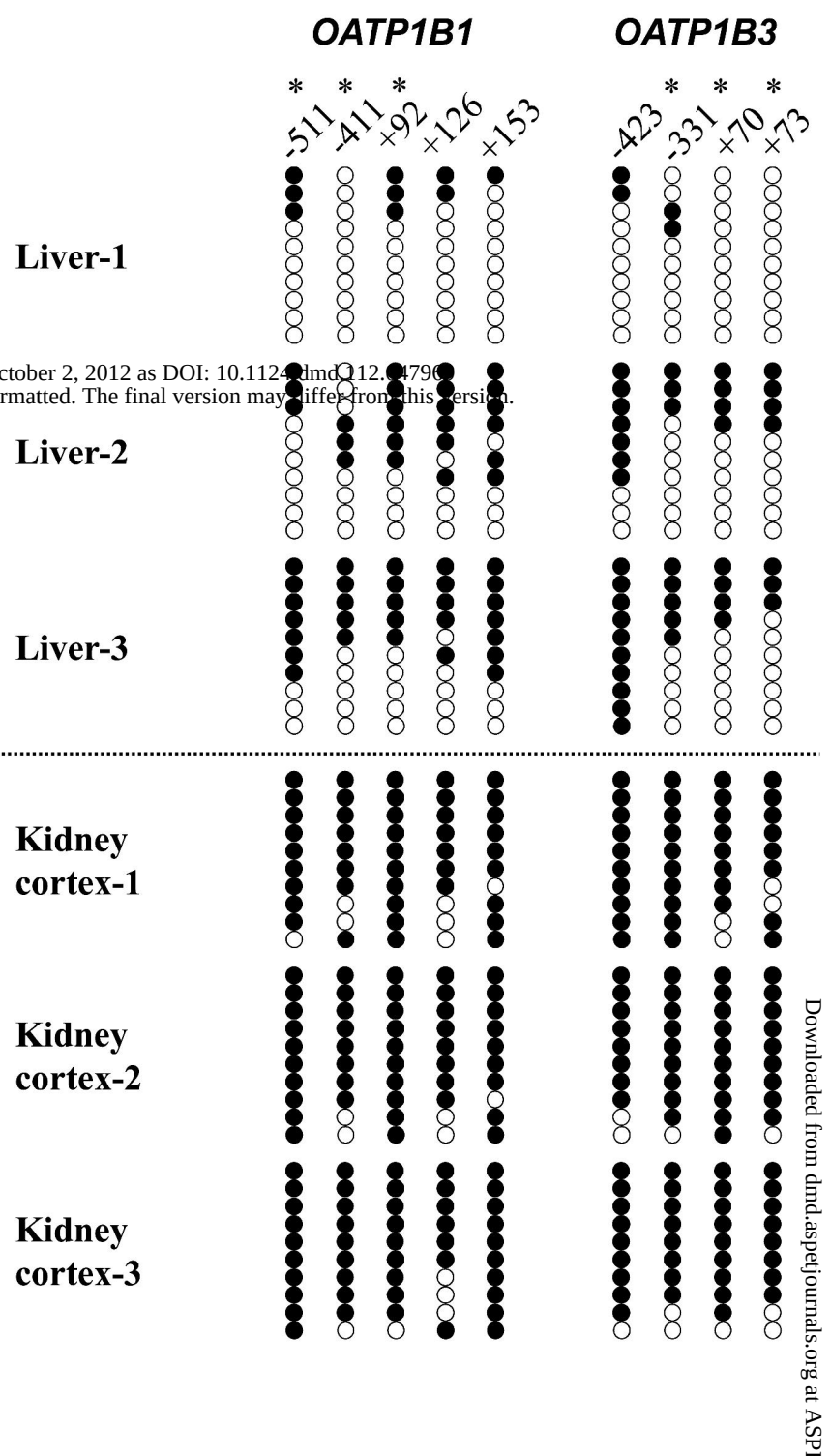

DMD Fast Forward. Published on October 2, 2012 as DOI: 10.1124/dmd.112.047969
This article has not been copyedited and formatted. The final version may differ from this version.

C